Absence of Transverse Tubules Contributes to Non-Uniform Ca^{2+} Wavefronts in Mouse and Human Embryonic Stem Cell–Derived Cardiomyocytes

Deborah K. Lieu,[1–3] Jing Liu,[1,2] Chung-Wah Siu,[1,4,5] Gregory P. McNerney,[3] Hung-Fat Tse,[4,5] Amir Abu-Khalil,[1,2] Thomas Huser,[3] and Ronald A. Li[2,4–6]

Mouse (m) and human embryonic stem cell-derived cardiomyocytes (hESC-CMs) are known to exhibit immature Ca^{2+} dynamics such as small whole-cell peak amplitude and slower kinetics relative to those of adult. In this study, we examined the maturity and efficiency of Ca^{2+}-induced Ca^{2+} release in m and hESC-CMs, the presence of transverse (t) tubules and its effects on the regional Ca^{2+} dynamics. In m and hESC-CMs, fluorescent staining and atomic force microscopy (AFM) were used to detect the presence of t-tubules, caveolin-3, amphiphysin-2 and colocalization of dihydropyridine receptors (DHPRs) and ryanodine receptors (RyRs). To avoid ambiguities, regional electrically-stimulated Ca^{2+} dynamics of single ESC-CMs, rather than spontaneously beating clusters, were measured using confocal microscopy. m and hESC-CMs showed absence of dyads, with neither t-tubules nor colocalization of DHPRs and RyRs. Caveolin-3 and amphiphysin-2, crucial for the biogenesis of t-tubules with robust expression in adult CMs, were also absent. Single m and hESC-CMs displayed non-uniform Ca^{2+} dynamics across the cell that is typical of CMs deficient of t-tubules. Local Ca^{2+} transients exhibited greater peak amplitude at the peripheral than at the central region for m (3.50 ± 0.42 vs. 3.05 ± 0.38) and hESC-CMs (2.96 ± 0.25 vs. 2.72 ± 0.25). Kinetically, both the rates of rise to peak amplitude and transient decay were faster for the peripheral relative to the central region. Immature m and hESC-CMs display unsynchronized Ca^{2+} transients due to the absence of t-tubules and gene products crucial for their biogenesis. Our results provide insights for driving the maturation of ESC-CMs.

Introduction

Adult cardiomyocytes (CMs) are unable to regenerate cells lost through disease or old age due to their inability to proliferate. Cell replacement therapy is a promising treatment, but is greatly hindered by limited cell source. Human (h) embryonic stem cells (ESCs) that are pluripotent and exhibit high proliferative capacity can be an unlimited source for CMs. However, human embryonic stem cell-derived cardiomyocytes (hESC-CMs) are physiologically different from their adult counterpart. They are smaller in size and electrophysiologically unstable with inefficient excitation–contraction coupling due to a relatively underdeveloped sarcoplasmic reticulum (SR), the intracellular Ca^{2+} store [1–3]. These immaturities and heterogeneous population of CMs at various differentiation stages or inclusion of different cell types can be substrates of arrhythmias. A better understanding of the basic biology of hESC-CMs is crucial for developing strategies for facilitated maturation to improve both the clinical efficacy and safety.

The main function of ventricular CMs is to generate efficient contractions for circulation. This is highly dependent upon the intracellular Ca^{2+} concentration, $[Ca^{2+}]_i$, that is available to bind to troponin C allowing actin–myosin cross-bridge cycling to generate contractions. This fast $[Ca^{2+}]_i$ increase depends on the efficiency of Ca^{2+}-induced Ca^{2+} release (CICR) that involves an initial Ca^{2+} influx through the

[1]Human Embryonic Cell Consortium, Stem Cell Program, [2]Department of Cell Biology and Human Anatomy, and [3]NSF Center for Biophotonics Science and Technology, University of California, Davis, California.
[4]Division of Cardiology, Department of Medicine, University of Hong Kong, Hong Kong.
[5]Stem Cell and Regenerative Medicine Programme, Heart, Brain, Hormone, and Healthy Aging Research Center, and [6]Institute of Pediatric Regenerative Medicine, Shriners Hospital for Children of North America, Sacramento, California.

activated L-type Ca^{2+} channels or dihydropyridine receptors (DHPRs) followed by Ca^{2+}-induced activation of the ryanodine receptors (RyRs) that results in Ca^{2+} release from the SR [4]. The efficiency of this positive feedback mechanism is dependent upon the diffusion distance between DHPRs and RyRs. Adult ventricular CMs circumvent this diffusion-limited problem by developing transverse (t) tubules, invaginations in the sarcolemmal membrane that concentrates DHPRs and brings them spatially close to RyRs residing on the SR membrane located deeper in the cytoplasm [5,6]. By physically minimizing the diffusion distance, RyRs in CMs even with large cross-sectional area can participate in CICR without a lag. The result is a synchronized, faster, and greater transient [Ca^{2+}]$_i$ increase from the peripheries to the center, creating a uniform Ca^{2+} wavefront across the transverse section with simultaneous recruitment of all SR, contrasting with a U-shaped Ca^{2+} wave propagation seen in a de-tubulated ventricular or atrial CMs [5], due to a time delay that is proportional to the diffusion distance squared in recruiting the Ca^{2+} stores at the cell center [7]. Fast and synchronized activation of RyRs translates into a greater Ca^{2+} transient amplitude, recruitment of more actin–myosin cross-bridge cycling, and generation of greater contractile force [5,8].

In this study, we examined the presence and the consequence of t-tubules on the colocalization of DHPRs with RyRs, and the resulting transient [Ca^{2+}]$_i$ spatiotemporal gradient in mouse (m) and hESC-CMs. Unlike several previous studies [1,9–11], *electrical stimulation of isolated, single ESC-CMs* rather than *spontaneously beating clusters* were studied to prevent gap junction-mediated electrical communications with neighboring cells that might contaminate genuine CICR mediated by DHPRs. Furthermore, while lipophilic staining is effective for identifying highly ordered arrangement of t-tubules in adult cells, debris or artifacts often show up as bright fluorescent spots that can be difficult to distinguish from genuine t-tubules if they are absent or have disorganized arrangements. Therefore, the highly sensitive technique atomic force microscopy (AFM) was employed to accurately probe the physical membrane topology of m and hESC-CMs. With AFM, debris would show up as elevations rather than invaginations in the membrane. We found that t-tubules were absent in m and hESC-CMs. These immature cells also did not exhibit colocalization of DHPRs and RyRs. Crucial proteins for t-tubule biogenesis were also absent. The resulting [Ca^{2+}]$_i$ change was a faster and higher magnitude of increase at the cell periphery than the central region similar to the immature fetal or neonatal CMs lacking t-tubules.

Materials and Methods

mESC culture and differentiation into mESC-CMs

D3 mESCs were cultured as previously described [12]. Briefly, mESCs were co-cultured with mouse embryonic fibroblasts (MEF) in Dulbecco's modified Eagle's medium (DMEM) (Cat. #11965; Invitrogen, Carlsbad, CA) supplemented with 15% fetal bovine serum (Hyclone), 1% nonessential amino acids (Invitrogen), 1 mmol/L ʟ-glutamine (Invitrogen), 0.1 mmol/L β-mercaptoethanol (Invitrogen), 0.5 U/mL penicillin (Invitrogen), 0.5 μg/mL streptomycin (Invitrogen), and 10 ng/mL leukemia inhibitory factor

(Sigma) at 37°C with 5% CO$_2$. Approximately 800 cells per 20 μL medium of hanging drops were allowed to incubate for 2 days to form embryoid bodies, and then grown in suspension for an additional 5 days before plating on 0.1% gelatin-coated Petri dishes. After 16–20 days post-differentiation, mESC-CMs were harvested and digested into single cells with collagenase II prior to plating for assessment of t-tubule formation, DHPRs colocalization with RyRs, presence of t-tubule biogenesis proteins, and local Ca^{2+} transients.

hESC culture and differentiation into hESC-CMs

hESCs, H1 line (WiCell) were cultured on MEF in DMEM/F12 (Invitrogen) supplemented (all from Invitrogen) with 15% knockout serum, 1% nonessential amino acids, 1 mmol/L ʟ-glutamine, 0.1 mmol/L β-mercaptoethanol, 0.5 U/mL penicillin, 0.5 μg/mL streptomycin, and 4 ng/mL basic fibroblast growth factor at 37°C with 5% CO$_2$. To initiate differentiation into hESC-CMs, hESC colonies were grown in suspension in low-attachment plates for 7 days in differentiation medium with the same composition as the mESC medium without β-mercaptoethanol. After 7 days of suspension, hESC embryoid bodies were plated in 0.1% gelatin-coated Petri dishes. After 40–50 days post-differentiation, hESC-CMs were identified by beating clusters and manually dissected out, then plated after digestion into single cells with collagenase II for assessment of t-tubule formation, DHPRs colocalization with RyRs, presence of t-tubule biogenesis proteins, and Ca^{2+} transients.

T-tubule fluorescent staining

For fluorescent t-tubule staining, m and hESC-CMs were incubated in 10 μM Di-8-ANEPPS (Invitrogen) for 10 min at room temperature, then washed for 10 min with phosphate-buffered saline (PBS). Images at the midplane of the cell height were taken with a Nikon laser scanning confocal microscope with a 60× oil immersion objective.

T-tubule detection with AFM

To probe the membrane topology, a Bioscope II (Veeco Metrology, Santa Barbara, CA) AFM with Microlever silicon nitride probe (MLCT-AUNM) tip D (spring constant [k] of 0.03 N/m) was used in contact mode to raster scan the surface of 0.05% glutaraldehyde-fixed m and hESC-CMs at room temperature in an aqueous environment at a scan speed of 0.5–0.7 Hz with 512 × 512 spatial resolution for a 10 μm region of interest. Images were generated either in 2D with cell topology variation shown in a gray scale or as a rendered 3D surface map using Nanoscope® Software.

Immunostaining of mESC-CMs and hESC-CMs

mESC-CMs and hESC-CMs were fixed with 4% paraformaldehyde for 15 min at room temperature and permeabilized with 0.2% saponin for 10 min at room temperature. Prior to overnight primary antibody incubation at 4°C, the cells were blocked in 1% BSA and 10% goat serum for 1 h at room temperature. DHPRs were labeled with rabbit Cav1.2 antibody (Sigma, St. Louis, MO) at 1:100. RyRs were labeled with mouse anti-RyR (Affinity Bioreagent) at 1:100.

Caveolin-3 (Santa Cruz Biotechnology, Santa Cruz, CA) and amphiphysin-2 (Santa Cruz Biotechnology) antibody concentrations were both 1:50. For DHPRs and RyRs staining, Alexa fluor 488 goat anti-rabbit IgG and Alexa fluor 546 goat anti-mouse IgG (Invitrogen, Carlsbad, CA) were used, respectively. Caveolin-3 and amphiphysin-2 slides were incubated in Alexa fluor 488 goat anti-mouse IgG (Invitrogen) for 1 h at room temperature. Finally, all nuclei were counterstained with Hoechst 33342 (Invitrogen). Slides were mounted using Prolong Gold Anti-fade reagent (Invitrogen).

Confocal Ca²⁺ imaging

To detect fast local Ca²⁺ changes in ESC-CMs, a spinning disk confocal microscope (Yokogawa CSU10) with high sampling frequency was used. Measurements using confocal microscopy allows for temporal as well as spatial $[Ca^{2+}]_i$ changes of m and hESC-CMs rather than global whole-cell $[Ca^{2+}]_i$ changes. *Single* m or hESC-CMs were incubated for 30 min at 37°C in 5 μM Fluo-4 (Invitrogen) with 0.02% pluronic (Invitrogen) in Hank's Buffered Salt Solution (Invitrogen). Single-cell Ca²⁺ transients of m or hESC-CMs at ~180 frames per second with a 40× microscope objective, stimulated by electric field of 40 V with 90 ms pulse duration at 0.2 Hz, were recorded at room temperature in Tyrode's solution consisting of (mM): 140 NaCl, 5 KCl, 1 MgCl₂, 2 CaCl₂, 10 glucose, and 10 HEPES at pH 7.4. The Ca²⁺ transient changes were quantified by the background subtracted fluorescent intensity changes normalized to the background subtracted baseline fluorescence using Image J. Specifically, the transient Ca²⁺ increases at the periphery and center of the cell due to electrical stimulations were compared. Paired Student's *t*-test analysis yielding $P < 0.05$ was considered to be statistically significant.

Results

mESC-CMs and hESC-CMs lack organized t-tubules that are present in adult CMs

To detect t-tubules, we initially used a fluorescent lipophilic dye, Di-8-ANEPPS, to stain three separately differentiated batches of >30 non-permeabilized m and hESC-CMs, and then imaged at their midplane in the *z*-axis using a laser scanning confocal microscope. Both m and hESC-CMs did not display brightly labeled spots in the central region of the cells (Fig. 1A and C), unlike our positive control of mature guinea pig ventricular CMs displaying an organized array of bright spots in the cellular midplane that are typical of CMs with t-tubules (Fig. 1E). For m and hESC-CMs, only their cellular periphery displayed bright fluorescence, indicative that the dye did bind to the cell membrane and that there was no presence of invaginated lipid membrane in their central region, thus, no organized t-tubules were present. To confirm these observations, we next physically scanned the three batches of >15 m and hESC-CM surface topography with AFM. Indeed, the surfaces of m and hESC-CMs were smooth with occasional appearance of the cytoskeleton beneath the sarcolemma in the AFM images (Fig. 1B and D). In contrast, adult guinea pig ventricular CMs known to have t-tubules exhibited invaginations that appeared periodically every 2 μm and coincided with the *z*-lines (Fig. 1F).
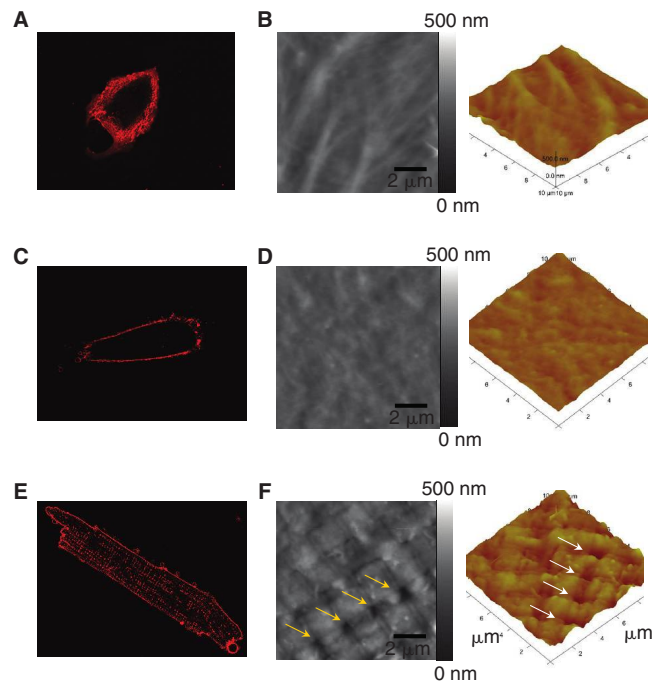

FIG. 1. T-tubule imaging of a mouse embryonic stem cell-derived cardiomyocyte (mESC-CM), a human ESC-CM (hESC-CM), and a mature ventricular CM. Di-8-ANEPPS confocal microscopic images of an mESC-CM (**A**) and an hESC-CM (**C**) did not show intracellular fluorescent spots like those in an adult guinea pig ventricular CM (**E**), suggesting the absence of t-tubules. The absence of t-tubules in ESC-CMs was further confirmed by AFM imaging of an adult guinea pig ventricular cardiomyocyte (**F**), showing regularly spaced pores in the sarcolemma that coincide with the *z*-lines, while mESC-CM (**B**) and hESC-CM (**D**) surface showed comparatively smoother topology with no presence of invaginations that are indicative of t-tubules.

DHPRs and RyRs do not colocalize in mESC-CMs and hESC-CMs

Double-staining of m (Fig. 2A) and hESC-CMs (Fig. 2B) for DHPRs and RyRs showed that the two crucial Ca²⁺-handling proteins did not colocalize. Clearly, dyads that are the signature of adult ventricular CMs were not observed. DHPRs were scattered diffusely throughout the derived CMs without any distinct pattern. RyRs were cytoplasmic and tended to localize around the periphery of the nuclei. This lack of colocalization was consistent with our findings that t-tubules were absent in m and hESC-CMs.

Caveolin-3 and amphiphysin-2 are absent in mESC-CMs and hESC-CMs

Since t-tubules were largely absent in both m and hESC-CMs, we next investigated the expression of two gene products, caveolin-3 and amphiphysin-2, that have been implicated to play crucial roles in t-tubule biogenesis. Figure 3 shows that neither caveolin-3 nor amphiphysin-2 could be detected in m and hESC-CMs. In stark contrast, adult ventricular CMs consistently showed intense positive staining for both.
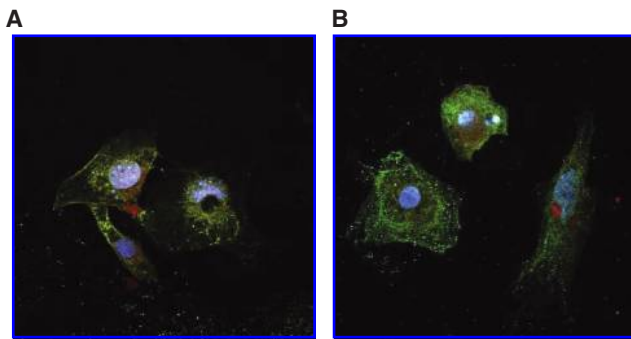
FIG. 2. Double immunostaining of DHPRs and RyRs in mouse and human embryonic stem cell-derived cardiomyocytes (mESC-CMs and hESC-CMs). DHPRs and RyRs showed lack of colocalization in mESC-CMs (**A**) and hESC-CMs (**B**). All cells were nuclear counterstained with Hoechst 33342.

mESC-CMs and hESC-CMs show non-uniform electrically-induced Ca²⁺ wavefronts

To explore the functional consequences due to the absence of t-tubules, single-cell local transient intracellular Ca^{2+} changes due to electrical stimuli were recorded by spinning disk confocal microscopy in Fluo-4-loaded m and hESC-CMs. Electrical stimulations of single ESC-CMs avoided gap junction-mediated electrical communications in spontaneously beating clusters. Time-lapsed images acquired at the z-axis midplane of a cell by confocal microscope were analyzed by converting the fluorescence from cell border to border into a spatial linescan versus time pseudo-colored for Ca^{2+} level to illustrate the Ca^{2+} wavefront propagation.

Both m and hESC-CMs exhibited a U-shaped Ca^{2+} wavefront typical of t-tubule-deficient CMs with a delayed increase in the central region of the cell relative to the peripheral region (Figs. 4A and 6A). These increases in $[Ca^{2+}]_i$

in m and hESC-CMs were lower in the central relative to the peripheral region as depicted by the color scale. Such U-shaped Ca^{2+} wavefronts were clearly different from the uniform wavefronts measured in adult ventricular CMs (Fig. 5A). This phenomenon of non-uniform wavefronts in immature mESC-CMs was also observed in coupled mESC-CMs (Fig. 5B). To quantify the regional differences in the fluorescence changes due to temporal Ca^{2+} fluxes, the peak amplitude, the maximum rate of intracellular Ca^{2+} increase, and the decay constant fitted to an exponential function for the Ca^{2+} transients were analyzed and compared (Figs. 4B,C and 6B,C). For mESC-CMs, their averaged peak Ca^{2+} transient amplitude was greater for the periphery relative to the center at 3.50 ± 0.42 and 3.05 ± 0.38, respectively ($P < 0.01$; n = 12). Their maximum transient rate of rise (V_{rise}) was faster at the peripheral (159 ± 39 s⁻¹) than the central region (130 ± 32 s⁻¹; $P < 0.01$). Their transient decay was also faster at the periphery as shown by their decay time constant (τ) at 0.88 ± 0.08 s⁻¹ and 1.13 ± 0.10 s⁻¹ for the central region ($P < 0.05$). Similar to mESC-CMs, the peak Ca^{2+} transient amplitude for the hESC-CMs at the periphery and the center were 2.96 ± 0.25 and 2.72 ± 0.25, respectively (n = 11; $P < 0.05$). Their transient rate of rise (V_{rise}) was also faster at the periphery (118 ± 18 s⁻¹) than the central region (96 ± 16 s⁻¹; $P < 0.05$). The transient decay was noticeably faster for the periphery (τ =1.34 ± 0.20 s⁻¹ vs. 1.84 ± 0.48 s⁻¹ for the central region), although this difference did not reach statistic significance ($P = 0.23$).

Discussion

Self-renewal and pluripotent ESCs that can differentiate into all cell types of the embryo proper is a potential unlimited source to derive CMs for cell replacement therapy; however, ESC-CMs are phenotypically and functionally immature relative to their adult counterparts [2,3,9,11,13,14]. We have previously shown at the whole-cell level that the CICR mechanism is not as efficient as that of adults due to the immature SR unable to fully contribute to the overall elevation
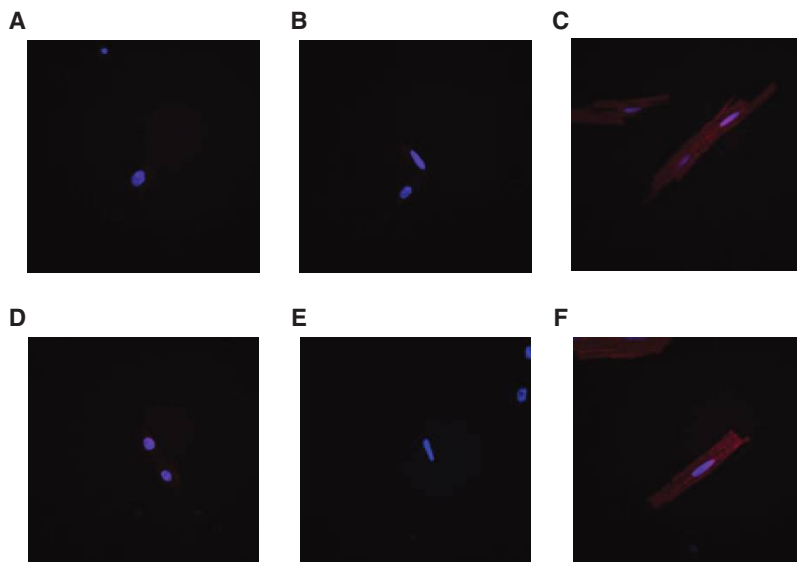

FIG. 3. Immunostaining of caveolin-3 and amphiphysin-2 in mouse embryonic stem cell-derived cardiomyocytes (mESC-CMs), human ESC-CMs (hESC-CMs), and mature adult CMs. Caveolin-3 was absent in both mESC-CMs (**A**) and hESC-CMs (**B**). Adult ventricular CMs were stained as positive control (**C**). Amphiphysin-2 was also deficient in mESC-CMs (**D**) and hESC-CMs (**E**). Amphiphysin-2 was also stained in adult ventricular CMs as positive control (**F**). All cell nuclei were counterstained with Hoechst 33342.
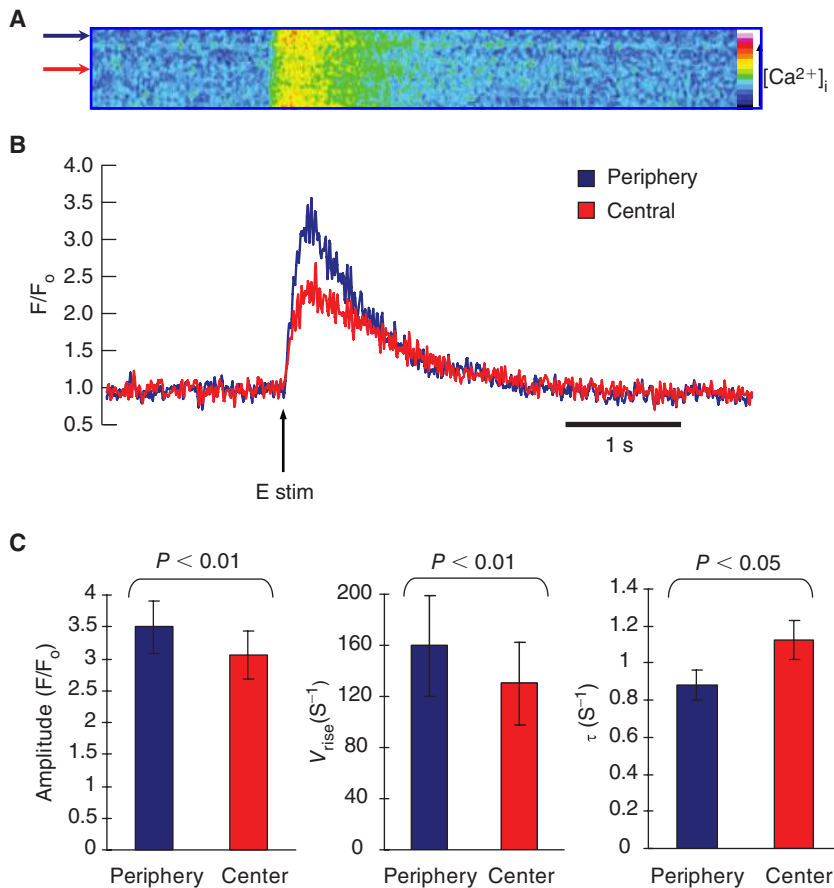
FIG. 4. Electrically-induced transient Ca²⁺ increase in mouse embryonic stem cell-derived cardiomyocytes (mESC-CMs). (**A**) Time progression linescans of pseudo-colored transient increase in intracellular Ca²⁺ across the midplane of a mESC-CM showed a U-shaped wavefront typical of CMs lacking t-tubules. (**B**) Quantified Ca²⁺ transient of linescans in **A**. The *arrow* indicates time of pulsed electrical stimulus. (**C**) The peak amplitude increase was statistically greater for the periphery relative to the center ($n = 12$). The transient rate of rise (V_{rise}) and the transient decay as shown by the decay time constant (τ) were both statistically faster at the peripheral than the central region. Data shown as mean ± SEM.

of [Ca²⁺]$_i$ [1]. In this study, we focused on t-tubules and local regional differences in Ca²⁺ transients.

T-tubules are invaginations about 200–300 nm in diameter occurring every ~2 µm at the sarcomere z-lines in the sarcolemmal membrane of adult mammalian ventricular CMs [5,6]. These structures concentrate the DHPRs and bring them spatially closer to the RyRs embedded in the SR membrane. Using fluorescent staining and AFM, we showed that t-tubules were absent from both m and hESC-CMs. Although some t-tubules have been detected in mESC-CM 28 days post-differentiation [15] and some or none in hESC-CMs 30 to 40 days post-appearance of beating areas by TEM [10,16], it is nonetheless clear that the frequency and the pattern of their occurrence do not compare to the extent seen in adult ventricular CMs. Therefore, generally the t-tubule development is still in its early stage like those of fetal or neonatal CMs [17,18]. Of note, any comparison of m and hESC-CMs should take into consideration any differences in their absolute ages and the relative gestational periods between the species. The time point that we have chosen for our mESC-CMs is 16–20 days, which is within the range of what are considered to be late stage in the literatures [13,19]. For hESC-CMs, the time point that we have chosen of 40–50 days was motivated by data of different stages in the literature and our own observations. Early (15–30 days) and late (55–110 days) stage hESC-CMs have been compared by Sartiani et al. [2]. Based on their data, there was not a significant change in the electrophysiological profile between days 57 and 110. Even between 25 and 57 days post-differentiation, various ion channel expression levels were already pretty similar. This means that an additional 50 days of culturing time did not promote significant improvements in hESC-CM maturity. Moreover, based on our observation, appearance of MLC2v-positive or
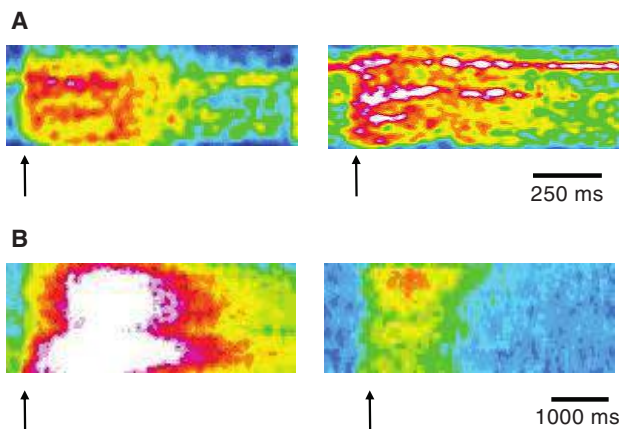

FIG. 5. Electrically-induced transient Ca²⁺ increase in adult guinea pig ventricular cardiomyocytes (CMs) and coupled cluster of mouse embryonic stem cell-derived CMs (mESC-CMs). (**A**) Time progression linescans show uniform Ca²⁺ wavefronts in mature adult ventricular CMs typical of CMs with t-tubules. (**B**) Time progression linescans of mESC-CMs in coupled cluster exhibited the same U-shaped Ca²⁺ wavefronts as the single mESC-CMs. The *arrows* indicate time of electrical stimulation.
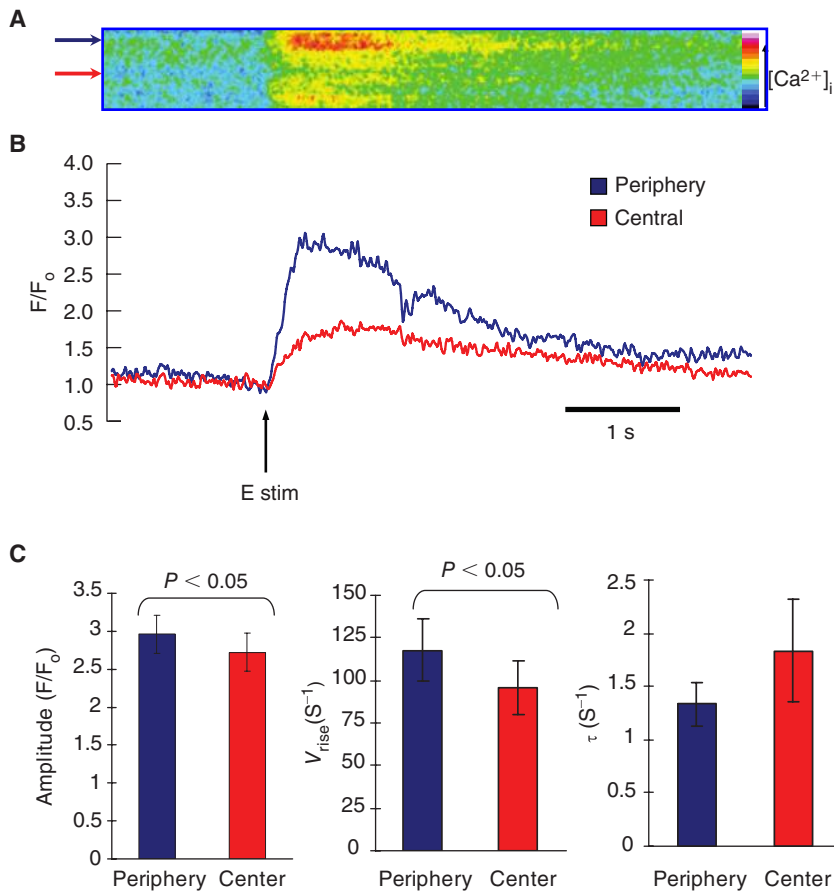
A

$[Ca^{2+}]_i$

B

Periphery
Central

E stim

1 s

C

$P < 0.05$

$P < 0.05$

Periphery Center

Periphery Center

Periphery Center

FIG. 6. Electrically-induced transient Ca^{2+} increase in human embryonic stem cell-derived cardiomyocytes (hESC-CMs). (**A**) Time progression linescans of pseudo-colored transient increase in intracellular Ca^{2+} across the midplane of a hESC-CM showed a U-shaped wavefront typical of CMs lacking t-tubules. (**B**) Quantified Ca^{2+} transient of linescans in **A**. The *arrow* indicates time of pulsed electrical stimulus. (**C**) The peak amplitude increase was statistically greater for the periphery relative to the center ($n = 11$). The transient rate of rise (V_{rise}) was statistically faster at the periphery than the central region. The transient decay was faster for the periphery as shown by their decay time constant (τ), but the difference did not reach statistical significance. Data shown as mean $\pm$ SEM.

ventricular CMs, which is the only CM type with presence of t-tubules, increased about 35 days post-differentiation in the beating areas. Hence, we have chosen a sampling time after appearance of ventricular hESC-CMs. Finally, we have decided to study hESC-CMs that have been in culture for a reasonable amount of time, but not too long for practicality of clinical application. If more mature hESC-CMs are more suitable for clinical practice, but these cells cannot reach the necessary maturity in a reasonable amount of culturing time, then facilitated induction of maturation may be a direction that needs to be explored.

Our stainings of m and hESC-CMs demonstrated no colocalization of DHPRs with RyRs, showing intracellular and periphery DHPRs and cytoplasmic RyRs that preferentially localize around the cell nuclei. This perinuclear pattern of RyRs was also observed by Sauer et al. in mESC-CMs at 5 to 11 days post-differentiation that progressed to the entire cytoplasmic compartment by the late stage [11]. This is consistent with our findings that t-tubules are absent in both m and hESC-CMs. Without t-tubules, there is no structure present to confine the DHPRs in a specific region and bring them spatially close to the RyRs residing on the SR membrane, leading to the lack of localization. Double-staining of DHPRs and RyRs in fetal rat CMs similarly exhibited no colocalization, with intracellular DHPRs that have been theorized to be in route to the subsarcolemma [17].

Caveolin has long been implicated to play a role in the formation of caveolae. T-tubule formation was thought to begin with the formation of caveolae chains that are unable

to undergo fission [20,21]. Caveolin-3, an isoform unique to muscle cells, is an integral membrane protein with a hairpin structure that can form oligomers and has the ability to bind to cholesterol to form highly ordered structures for spatially confining integral proteins [20,21]. Amphiphysin-2 localized in the t-tubules is another membrane-associated protein with a BAR domain at the N-terminus, which is named for its presence in the vertebrate Bin1 and Amphiphysins and in the *Saccharomyces cerevisiae* Rvs proteins [22], that can sense the membrane curvature, binds and evaginates the membrane even in nonmuscle cells [22–24], suggesting that amphiphysin-2 may be an initiator in t-tubule formation. Neither caveolin-3 nor amphiphysin-2 was expressed in m and hESC-CMs; our laboratory is currently investigating whether their forced expression may drive structural maturation to facilitate Ca^{2+} handling.

For m and hESC-CMs, the periphery displayed statistically greater peak amplitude increase and faster rise time and exponential decay constant relative to the center. We and Satin et al. have also observed similar regional differences in small clusters of m and hESC-CMs [10]. Similarly, asynchronous Ca^{2+} wavefronts have been observed in immature fetal or newborn ventricular CMs [18]. The observed slower rate of rise and smaller amplitude increase are due to the time needed for the Ca^{2+} influx through DHPRs to diffuse from the border to recruit the RyRs residing on the SR membrane located deep inside the cytosol to activate the CICR mechanism. Although statistical significance has been reached, our regional differences are less than those

seen in fetal or neonatal, atrial or de-tubulated adult ventricular CMs [17,18,25–27]. The smaller differences may be due to the intrinsically smaller cell size of ESC-CMs. This small cross-sectional area or shorter diffusion distance from the cell border to the center is further diminished by the 2D culture condition that is routinely in practice. Planer culture condition has been shown to result in cellular polarity, such that the colocalization pattern of HSP90 and eNOS differs between 2D and 3D culture environments due to the free cellular surface lacking cell–cell interaction in the 2D condition [28]. We chose to detect t-tubules in single cells to match the state of ESC-CMs in our Ca^{2+} imaging experiments. With ESC-CMs randomly oriented and not exhibiting rod-shape morphology like the fetal CMs in vivo, we had typically selected lines straight across a cell in the XY-plane that had the shortest distance; however, the diffusion distance in these immature cells with small cross-sectional area is furthered diminished by the 2D culture environment. Their shortest diffusion distance was actually in the z-axis or the cell height with typical distance of ~6 μm relative to our linescan recording across the cells at 18.0 ± 1.4 and 16.6 ± 1.6 μm for mESC-CM and hESC-CMs, respectively. Therefore, although how we chose the region of interest is important, the more critical point is that the Ca^{2+} in the central region most likely diffused in from the top of the cells rather than from the sides. Since the diffusion time is proportional to the diffusion distance squared [7], the diffusion-limited effect may not be as pronounced at the current diffusion distance for ESC-CMs with a small cross-sectional area compared to that of more mature CMs in vivo with cross-sectional area of 10 μm or more. Thus, further investigations of the effect of 3D culturing are warranted, and may lead to optimized culturing methods to facilitate maturation for clinical applications. Another experimental limitation is that all Ca^{2+} transients were elicited with a field stimulator that may excite multiple sites rather than point stimulation with a micropipette; however, our conclusion remains valid since the spread of depolarization depends on the intrinsically faster Na^+ channels with a lower activation threshold than the DHPRs, followed by the activation of DHPRs that triggers the CICR process.

Although hESC-CMs have been shown to functionally integrate with resident CMs in vitro and in vivo [29], the transplanted ESC-CMs with asynchronous Ca^{2+} wavefronts or weaker contractile force may not augment cardiac contraction enough to improve blood circulation. Moreover, the weak contractile force may create a mechanical strain imbalance for the resident CMs at the interface between the native and the newly introduced ESC-CMs, which could result in the advancement of pathological hypertrophy in the heart. Therefore, improvements in the excitation–contraction coupling such as t-tubules and the contractile force in ESC-CMs are desirable.

Interestingly, CMs with smaller cross-sectional areas such as mature avian or fish and immature fetal or neonatal mammalian CMs do not possess t-tubules [30]. Even those atrial cells that do possess irregular internal transverse-axial tubular system, a modified t-tubule system, tend to have a greater mean diameter than those that do not [31]. The lack of t-tubules in these CMs may be dependent on the cell cross-sectional area and/or the diffusion distance. Therefore, whether t-tubules development is triggered by an increase in cell size to compensate for the increase in diffusion distance

or initiation of t-tubule development allows for cellular hypertrophy is an interesting issue that may shed important insights for deriving more functionally viable, mature CMs for cell transplantation or drug screening.

Acknowledgments

Author Disclosure Statement

No competing financial interests exist.

References

1. Liu J, JD Fu, CW Siu and RA Li. (2007). Functional sarcoplasmic reticulum for calcium-handling of human embryonic stem cell-derived cardiomyocytes: insights for driven maturation. Stem Cells 25:3038–3044.
2. Sartiani L, E Bettiol, F Stillitano, A Mugelli, E Cerbai and ME Jaconi. (2007). Developmental changes in cardiomyocytes differentiated from human embryonic stem cells: a molecular and electrophysiological approach. Stem Cells 25:1136–1144.
3. Itzhaki I, J Schiller, R Beyar, J Satin and L Gepstein. (2006). Calcium handling in embryonic stem cell-derived cardiac myocytes: of mice and men. Ann N Y Acad Sci 1080:207–215.
4. Bers DM. (2002). Cardiac excitation–contraction coupling. Nature 415:198–205.
5. Brette F and C Orchard. (2003). T-tubule function in mammalian cardiac myocytes. Circ Res 92:1182–1192.
6. Brette F and C Orchard. (2007). Resurgence of cardiac t-tubule research. Physiology (Bethesda) 22:167–173.
7. Song LS, S Guatimosim, L Gomez-Viquez, EA Sobie, A Ziman, H Hartmann and WJ Lederer. (2005). Calcium biology of the transverse tubules in heart. Ann N Y Acad Sci 1047:99–111.
8. Louch WE, V Bito, FR Heinzel, R Macianskiene, J Vanhaecke, W Flameng, K Mubagwa and KR Sipido. (2004). Reduced synchrony of Ca^{2+} release with loss of T-tubules-a comparison to Ca^{2+} release in human failing cardiomyocytes. Cardiovasc Res 62:63–73.
9. Kapur N and K Banach. (2007). Inositol-1,4,5-trisphosphate-mediated spontaneous activity in mouse embryonic stem cell-derived cardiomyocytes. J Physiol 581:1113–1127.
10. Satin J, I Itzhaki, S Rapoport, EA Schroder, L Izu, G Arbel, R Beyar, CW Balke, J Schiller and L Gepstein. (2008). Calcium handling in human embryonic stem cell derived cardiomyocytes. Stem Cells 26:1961–1072.
11. Sauer H, T Theben, J Hescheler, M Lindner, MC Brandt and M Wartenberg. (2001). Characteristics of calcium sparks in cardiomyocytes derived from embryonic stem cells. Am J Physiol Heart Circ Physiol 281:H411–H421.
12. Wobus AM, K Guan, HT Yang and KR Boheler. (2002). Embryonic stem cells as a model to study cardiac, skeletal muscle, and vascular smooth muscle cell differentiation. Methods Mol Biol 185:127–156.

13. Boheler KR, J Czyz, D Tweedie, HT Yang, SV Anisimov and AM Wobus. (2002). Differentiation of pluripotent embryonic stem cells into cardiomyocytes. Circ Res 91:189–201.

14. Satin J, I Itzhaki, S Rapoport, EA Schroder, L Izu, G Arbel, R Beyar, CW Balke, J Schiller and L Gepstein. (2008). Calcium handling in human embryonic stem cell-derived cardiomyocytes. Stem Cells 26:1961–1972.

15. Baharvand H, A Piryaei, R Rohani, A Taei, MH Heidari and A Hosseini. (2006). Ultrastructural comparison of developing mouse embryonic stem cell- and in vivo-derived cardiomyocytes. Cell Biol Int 30:800–807.

16. Snir M, I Kehat, A Gepstein, R Coleman, J Itskovitz-Eldor, E Livne and L Gepstein. (2003). Assessment of the ultrastructural and proliferative properties of human embryonic stem cell-derived cardiomyocytes. Am J Physiol Heart Circ Physiol 285:H2355–H2363.

17. Seki S, M Nagashima, Y Yamada, M Tsutsuura, T Kobayashi, A Namiki and N Tohse. (2003). Fetal and postnatal development of Ca^{2+} transients and Ca^{2+} sparks in rat cardiomyocytes. Cardiovasc Res 58:535–548.

18. Haddock PS, WA Coetzee, E Cho, L Porter, H Katoh, DM Bers, MS Jafri and M Artman. (1999). Subcellular $[Ca^{2+}]_i$ gradients during excitation-contraction coupling in newborn rabbit ventricular myocytes. Circ Res 85:415–427.

19. Fu JD, J Li, D Tweedie, HM Yu, L Chen, R Wang, DR Riordon, SA Brugh, SQ Wang, KR Boheler and HT Yang. (2006). Crucial role of the sarcoplasmic reticulum in the developmental regulation of Ca^{2+} transients and contraction in cardiomyocytes derived from embryonic stem cells. FASEB J 20:181–183.

20. Carozzi AJ, E Ikonen, MR Lindsay and RG Parton. (2000). Role of cholesterol in developing t-tubules: analogous mechanisms for t-tubule and caveolae biogenesis. Traffic 1:326–341.

21. Parton RG, AJ Carozzi and J Gustavsson. (2000). Caves and labyrinths: caveolae and transverse tubules in skeletal muscle. Protoplasma 212:15–23.

22. Casal E, L Federici, W Zhang, J Fernandez-Recio, EM Priego, RN Miguel, JB DuHadaway, GC Prendergast, BF Luisi and ED Laue. (2006). The crystal structure of the BAR domain from human Bin1/amphiphysin II and its implications for molecular recognition. Biochemistry 45:12917–12928.

23. Butler MH, C David, GC Ochoa, Z Freyberg, L Daniell, D Grabs, O Cremona and P De Camilli. (1997). Amphiphysin II (SH3P9; BIN1), a member of the amphiphysin/Rvs family, is concentrated in the cortical cytomatrix of axon initial segments and nodes of ranvier in brain and around t tubules in skeletal muscle. J Cell Biol 137:1355–1367.

24. Lee E, M Marcucci, L Daniell, M Pypaert, OA Weisz, GC Ochoa, K Farsad, MR Wenk and P De Camilli. (2002). Amphiphysin 2 (Bin1) and t-tubule biogenesis in muscle. Science 297:1193–1196.

25. Mackenzie L, MD Bootman, MJ Berridge and P Lipp. (2001). Predetermined recruitment of calcium release sites underlies excitation-contraction coupling in rat atrial myocytes. J Physiol 530:417–429.

26. Mackenzie L, HL Roderick, MJ Berridge, SJ Conway and MD Bootman. (2004). The spatial pattern of atrial cardiomyocyte calcium signalling modulates contraction. J Cell Sci 117:6327–6337.

27. Brette F, S Despa, DM Bers and CH Orchard. (2005). Spatiotemporal characteristics of SR Ca(2+) uptake and release in detubulated rat ventricular myocytes. J Mol Cell Cardiol 39:804–812.

28. Di Felice V, F Cappello, A Montalbano, NM Ardizzone, A De Luca, F Macaluso, D Amelio, MC Cerra and G Zummo. (2007). HSP90 and eNOS partially co-localize and change cellular localization in relation to different ECM components in 2D and 3D cultures of adult rat cardiomyocytes. Biol Cell 99:689–699.

29. Xue T, HC Cho, FG Akar, SY Tsang, SP Jones, E Marban, GF Tomaselli and RA Li. (2005). Functional integration of electrically active cardiac derivatives from genetically engineered human embryonic stem cells with quiescent recipient ventricular cardiomyocytes: insights into the development of cell-based pacemakers. Circulation 111:11–20.

30. Shiels HA and E White. (2005). Temporal and spatial properties of cellular Ca^{2+} flux in trout ventricular myocytes. Am J Physiol Regul Integr Comp Physiol 288:R1756–R1766.

31. Kirk MM, LT Izu, Y Chen-Izu, SL McCulle, WG Wier, CW Balke and SR Shorofsky. (2003). Role of the transverse-axial tubule system in generating calcium sparks and calcium transients in rat atrial myocytes. J Physiol 547:441–451.

Address correspondence to:
Dr. Ronald A. Li
Stem Cell Program
University of California, Davis
Shriners Hospital for Children
Room 650
2425 Stockton Boulevard
Sacramento, CA 95817

E-mail: ronaldli@ucdavis.edu

or

Dr. Deborah K. Lieu
Stem Cell Program
University of California, Davis
Shriners Hospital for Children
Room 650
2425 Stockton Boulevard
Sacramento, CA 95817

E-mail: dklieu@ucdavis.edu

This article has been cited by:

1. Scott D. Lundy, Wei-Zhong Zhu, Michael Regnier, Michael A. Laflamme. 2013. Structural and Functional Maturation of Cardiomyocytes Derived from Human Pluripotent Stem Cells. *Stem Cells and Development* **22**:14, 1991-2002. [Abstract] [Full Text HTML] [Full Text PDF] [Full Text PDF with Links] [Supplemental Material]

2. Sara S Nunes, Jason W Miklas, Jie Liu, Roozbeh Aschar-Sobbi, Yun Xiao, Boyang Zhang, Jiahua Jiang, Stéphane Massé, Mark Gagliardi, Anne Hsieh, Nimalan Thavandiran, Michael A Laflamme, Kumaraswamy Nanthakumar, Gil J Gross, Peter H Backx, Gordon Keller, Milica Radisic. 2013. Biowire: a platform for maturation of human pluripotent stem cell–derived cardiomyocytes. *Nature Methods* **10**:8, 781-787. [CrossRef]

3. Maggie Zi Ying Chow, Lin Geng, Chi-Wing Kong, Wendy Keung, Jacky Chun-Kit Fung, Kenneth R. Boheler, Ronald A. Li. Epigenetic Regulation of the Electrophysiological Phenotype of Human Embryonic Stem Cell-Derived Ventricular Cardiomyocytes: Insights for Driven Maturation and Hypertrophic Growth. *Stem Cells and Development*, ahead of print. [Abstract] [Full Text HTML] [Full Text PDF] [Full Text PDF with Links] [Supplemental Material]

4. Clay W Scott, Matthew F. Peters, Yvonne P. Dragan. 2013. Human induced pluripotent stem cells and their use in drug discovery for toxicity testing. *Toxicology Letters* **219**:1, 49-58. [CrossRef]

5. Claire Robertson, David D. Tran, Steven C. George. 2013. Concise Review: Maturation Phases of Human Pluripotent Stem Cell-Derived Cardiomyocytes. *STEM CELLS* **31**:5, 829-837. [CrossRef]

6. Deborah K. Lieu, Irene C. Turnbull, Kevin D. Costa, Ronald A. Li. 2012. Engineered human pluripotent stem cell-derived cardiac cells and tissues for electrophysiological studies. *Drug Discovery Today: Disease Models* **9**:4, e209-e217. [CrossRef]

7. R. D. Kirkton, N. Bursac. 2012. Genetic engineering of somatic cells to study and improve cardiac function. *Europace* **14**:suppl 5, v40-v49. [CrossRef]

8. Adriana Blazeski, Renjun Zhu, David W. Hunter, Seth H. Weinberg, Kenneth R. Boheler, Elias T. Zambidis, Leslie Tung. 2012. Electrophysiological and contractile function of cardiomyocytes derived from human embryonic stem cells. *Progress in Biophysics and Molecular Biology* **110**:2-3, 178-195. [CrossRef]

9. Yuji Shiba, Sarah Fernandes, Wei-Zhong Zhu, Dominic Filice, Veronica Muskheli, Jonathan Kim, Nathan J. Palpant, Jay Gantz, Kara White Moyes, Hans Reinecke, Benjamin Van Biber, Todd Dardas, John L. Mignone, Atsushi Izawa, Ramy Hanna, Mohan Viswanathan, Joseph D. Gold, Michael I. Kotlikoff, Narine Sarvazyan, Matthew W. Kay, Charles E. Murry, Michael A. Laflamme. 2012. Human ES-cell-derived cardiomyocytes electrically couple and suppress arrhythmias in injured hearts. *Nature* **489**:7415, 322-325. [CrossRef]

10. Michelangelo Paci, Laura Sartiani, Martina Del Lungo, Marisa Jaconi, Alessandro Mugelli, Elisabetta Cerbai, Stefano Severi. 2012. Mathematical modelling of the action potential of human embryonic stem cell derived cardiomyocytes. *BioMedical Engineering OnLine* **11**:1, 61. [CrossRef]

11. Kwong-Man Ng, Yau-Chi Chan, Yee-Ki Lee, Wing-Hon Lai, Ka-Wing Au, Man-Lung Fung, Chung-Wah Siu, Ronald A. Li, Hung-Fat Tse. 2011. Cobalt Chloride Pretreatment Promotes Cardiac Differentiation of Human Embryonic Stem Cells Under Atmospheric Oxygen Level. *Cellular Reprogramming* **13**:6, 527-537. [Abstract] [Full Text HTML] [Full Text PDF] [Full Text PDF with Links]

12. Samir Awasthi, Dennis L. Matthews, Ronald A. Li, Nipavan Chiamvimonvat, Deborah K. Lieu, James W. Chan. 2011. Label-free identification and characterization of human pluripotent stem cell-derived cardiomyocytes using second harmonic generation (SHG) microscopy. *Journal of Biophotonics* n/a-n/a. [CrossRef]

13. Ellen Poon, Chi-wing Kong, Ronald A. Li. 2011. Human Pluripotent Stem Cell-Based Approaches for Myocardial Repair: From the Electrophysiological Perspective. *Molecular Pharmaceutics* 110908085036072. [CrossRef]

14. James E. Hudson, Wolfram-Hubertus Zimmermann. 2011. Tuning Wnt-signaling to enhance cardiomyogenesis in human embryonic and induced pluripotent stem cells. *Journal of Molecular and Cellular Cardiology* **51**:3, 277-279. [CrossRef]

15. Yee-Ki Lee, Kwong-Man Ng, Wing-Hon Lai, Yau-Chi Chan, Yee-Man Lau, Qizhou Lian, Hung-Fat Tse, Chung-Wah Siu. 2011. Calcium Homeostasis in Human Induced Pluripotent Stem Cell-Derived Cardiomyocytes. *Stem Cell Reviews and Reports* . [CrossRef]

16. Yongming Ren, Min Young Lee, Simon Schliffke, Jere Paavola, Peter J. Amos, Xin Ge, Mingyu Ye, Shenjun Zhu, Grant Senyei, Lawrence Lum, Barbara E. Ehrlich, Yibing Qyang. 2011. Small molecule Wnt inhibitors enhance the efficiency of BMP-4-directed cardiac differentiation of human pluripotent stem cells. *Journal of Molecular and Cellular Cardiology* . [CrossRef]

17. Yee-Ki Lee, Kwong-Man Ng, Wing-Hon Lai, Cornelia Man, Deborah K Lieu, Chu-Pak Lau, Hung-Fat Tse, Chung-Wah Siu. 2011. Ouabain facilitates cardiac differentiation of mouse embryonic stem cells through ERK1/2 pathway. *Acta Pharmacologica Sinica* **32**:1, 52-61. [CrossRef]

18. Kwong-Man Ng, Yee-Ki Lee, Yau-Chi Chan, Wing-Hon Lai, Man-Lung Fung, Ronald A. Li, Chung-Wah Siu, Hung-Fat Tse. 2010. Exogenous expression of HIF-1α promotes cardiac differentiation of embryonic stem cells. *Journal of Molecular and Cellular Cardiology* **48**:6, 1129-1137. [CrossRef]